

Sputter ion pump element pumping speed measurement with the help of a Monte Carlo code

Medição da velocidade de bombeamento de elemento de bomba iônica com auxílio de código Monte Carlo

Rafael M. Seraphim¹, Reginaldo O. Ferraz¹, Thiago M. Rocha¹, Gustavo R. Gomes¹, Milton B. Silva¹, Helio Gazetta Filho¹

ABSTRACT

As part of the design of the vacuum system of a new Synchrotron Light Source for Brazil – SIRIUS, the Vacuum Group from the Brazilian Synchrotron Light Laboratory (LNLS) proposed the pumping speed study of a sputter ion pump element assembled inside the vacuum chamber. This configuration aims to reduce components attached to the chamber enabling an easier alignment procedure and a conductance enhancement to pumped gases. The study was carried out by experimental measurements and numerical simulations using Monte Carlo method. The measurements and Monte Carlo calculations results presented a good agreement, with errors less than 10%. Further, inserting the element in the vacuum chamber enhanced maximum pumping speed when compared with the manufacturer's data, due to the conductance's increase for gases.

Keywords: Sputter ion pump; Pumping speed; Monte Carlo.

RESUMO

Como parte do projeto do sistema de vácuo de uma nova fonte de luz síncrotron para o Brasil - SIRIUS, o Grupo de Vácuo do Laboratório Nacional de Luz Síncrotron (LNLS) propôs o estudo da velocidade de bombeamento de um elemento de bomba iônica posicionado no interior da câmara de vácuo. Esta configuração visa facilitar o processo de alinhamento das câmaras por reduzir o número de componentes acoplados a ela e também aumentar a condutância para o bombeamento dos gases. O estudo foi conduzido mediante medidas experimentais e simulações numéricas utilizando o método de Monte Carlo. Os resultados dos experimentos e cálculos baseados no método de Monte Carlo mostraram grande concordância, com erros iguais ou inferiores a 10%. Além disso, a inserção do elemento na câmara de vácuo gerou uma velocidade de bombeamento máxima superior ao nominal especificado pelo fabricante da bomba iônica, fato este justificado pelo aumento da condutância para os gases.

Palavras-chave: Bomba iônica; Velocidade de bombeamento; Monte Carlo.

¹Laboratório Nacional de Luz Síncrotron – Grupo de Vácuo – Campinas (SP) – Brasil

Correspondence author: Thiago M. Rocha – LNLS – Grupo de Vácuo – C.P. 6192 – CEP 13084-971 Campinas(SP) – Brazil
Email: tmrocha88@gmail.com

Received: 08/29/2011 **Approved:** 06/15/2015

INTRODUCTION

The Brazilian Synchrotron Light Laboratory (LNLS) started the design of a new synchrotron light source for Brazil – SIRIUS⁽¹⁾. The design of the machine will be divided by subsystem, which has different engineering groups responsible for each one. The Vacuum Group already started the studies to design the vacuum system.

From the vacuum point of view, these machines are namely conductance limited, because of their small cross section dimensions and long length. Therefore, the most difficult thing regarding the vacuum system design is provide enough pumping speed in needed places of the machine. Generally, this is obtained by using lumped or distributed pumps. The last one, is commonly achieved using the so called “non evaporable getters” (NEG) or, in some specific cases, using distributed sputter ion pumps (SIPs). However, the use of NEG implies heating the vacuum chambers to temperatures higher than 150 °C for activation, which will not be allowed because of the permanent magnets to be used in Sirius, making the distributed SIPs an alternative. Then, the aim of this work is measure the pumping speed of a SIP element assembled inside of a chamber without its conventional body or pocket and support the results by using a Monte Carlo method⁽²⁾. In this way, we will understand the pump efficiency when installed directly in the chamber, increasing the conductance for the gases and reducing the quantity of heavy components attached to the chamber.

EXPERIMENTAL METHOD

EXPERIMENTAL SETUP

A 20 L/s ion pump element was taken for pumping speed measurement. Table 1 shows the parameters of the pump element under studies. The measurement was carried out using a special assembly (Assembly A, see Fig.1), which has an intentionally complex geometry, since it is important to distinguish the behavior of the pumping element from the conventional assembly. In addition, the experimental setup comprises three calibrated cold cathode gauges and an ultrahigh vacuum (UHV) leak rate valve to control the injected gas, which was the 99.999% Nitrogen. The measurements were based on the orifice method⁽³⁾, where the gas

Table 1: Parameters of the pump element under studies.

Parameter	Description
Anode	
Radius	9 mm
Length	14 mm
Overall	
Width	95 mm
Length	152 mm
Gap	7 mm
No. cells	32
Magnetic filed	1800 G

flow is determined by means of the pressure drop across an orifice with known conductance (3.4 L/s N₂ equivalent). Due to the complex geometry and the pressure gradient inside the chamber, a third gauge was used to help defining the chamber's pressure profile. Moreover, a Monte Carlo based code (MOLFLOW+)⁽²⁾, gently provided by Roberto Kersevan was used to numerically estimate the pressure profile inside the chamber and support the results obtained with the measurements.

However, to validate the software's calculations, an auxiliary experiment was prepared (Assembly B, see Fig. 2). This assembly has a stainless steel vacuum chamber with standardized dimensions^(3,4) and a known conductance (3.4 L/s N₂) placed between the halves. Further, two Leybold Extractor IE514 vacuum gauges and an ultra high vacuum leak rate valve comprise the whole assembly. Also, the goal was evaluate the pumping speed of a 20 L/s ion pump element (same parameters as shown in Table 1).

EXPERIMENTAL PROCEDURE

Before beginning the pumping speed measurements, the experimental setups were submitted to a bake-out procedure to degas the parts and achieve a pressure in the ultrahigh vacuum range. Figure 3 illustrates the pump down curve for the bake-out procedure of Assembly's A first measurement test, whose curve's behavior can be used as a reference for the bake-out profile of the other measurements. The system was maintained in 200 °C for 48 hours, with ramps of heating and cooling of 12 hours. The

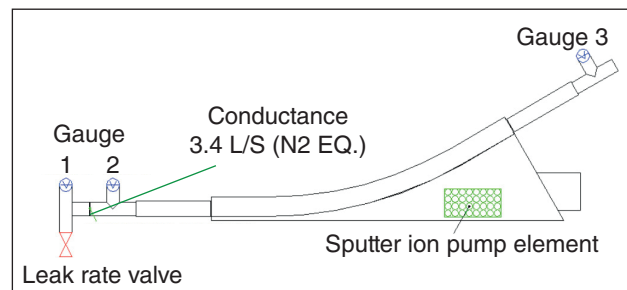


Figure 1: Schematic drawing of the Assembly A. Gauges 1, 2 and 3: calibrated cold cathode gauge; SIP: 20 L/s element.

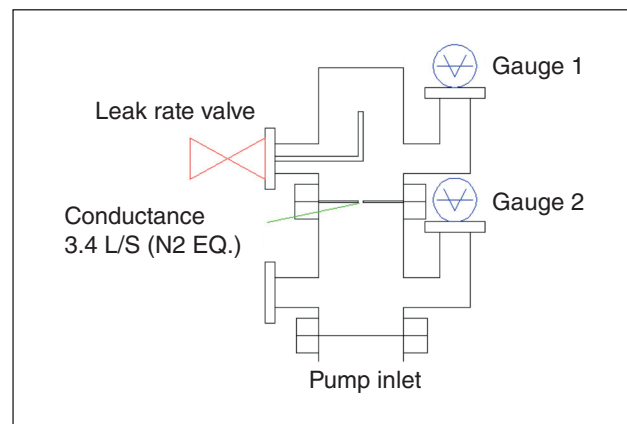


Figure 2: Schematic drawing of Assembly B. Gauges 1 and 2: calibrated extractor gauge.

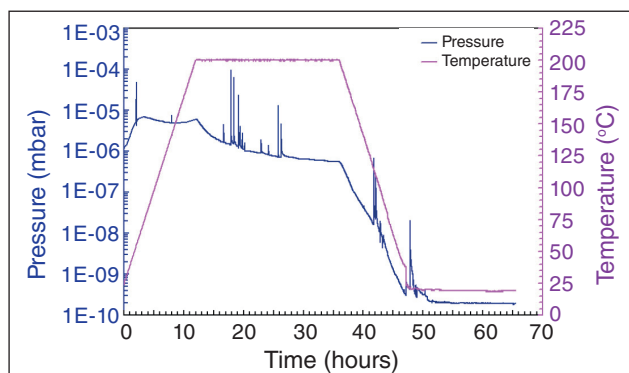


Figure 3: Pump down curve during the bake-out.

experiment of Assembly A, whose results will be shown in this paper, achieved a final pressure of about 5×10^{-10} mbar (N_2 eq.). An analogous bake-out procedure was adopted for Assembly B and the final attained pressure was in the low 10^{-10} mbar range (N_2 eq.). The attained pressures of both Assemblies A and B allowed us to measure the pumping speed of the ion pump element from about 10^{-9} till 10^{-6} mbar.

The measurements starting from pressures of 10^{-9} mbar are reasonable but not optimum, since it would be great to measure the pumping speed in pressures as low as 10^{-10} mbar. However, to take measurements at this pressure level, the final attained pressure after bake-out should be at the 10^{-11} mbar range, which was not possible for both Assemblies A and B.

The measurements were carried out adopting the following sequence:

1. Take note of the final attained pressure at the chamber;
2. Adjust the nitrogen flux (cylinder manometer pressure at 1379 mbar).
3. Progressive opening of the leak rate valve until the desired base pressure at the reference gauge (10 times higher than the final attained pressure⁽³⁾) is achieved.
4. Wait 10 minutes for pressure stabilization at the vacuum chamber and record the data. Take note of pressures shown by calibrated vacuum gauges and SIP power source voltage and current.
5. Progressive opening of the leak rate valve until the desirable pressure at the reference gauge is doubled.

The above procedure was repeated until achieve a maximum established pressure at the chamber, which was 5.0×10^{-5} mbar (N_2 eq.), since this pressure value would not harm the gauges.

From the recorded values, it was possible to calculate the gas flow through the orifice of known conductance (C) and, as a consequence, the pumping speed (S) of the SIP element, according to⁽¹⁾.

$$S = C \left(\frac{P_{inj}}{P_{pump}} - 1 \right) \quad (1)$$

where:

P_{inj} is the pressure where the gas is injected and P_{pump} is the pressure at the side of the pumping place, which in the case of Assembly A was the pressure measured by gauge 3.

RESULTS AND DISCUSSION

The use of a standardized procedure for measuring the pumping speed was important to validate the numerical calculations using the Monte Carlo method.

Table 2 presents the results for the measurements and Monte Carlo calculations regarding Assembly B. The uncertainties at the pressure measurement are $\pm 20\%$ due to the gauge calibration. The pressure of gauge 2 (closer to the pumping element) was varied from low 10^{-9} mbar until 4×10^{-6} mbar in order to analyze the pumping speed dependency with pressure.

Table 2: Comparison between the calculated pumping speed from measurements and Monte Carlo calculations for Assembly B.

Gauge 1	Gauge 1 MC	Gauge 2	Gauge 2 MC	Q	S
mbar	mbar	mbar	mbar	mbar*L/s	L/s
5.58×10^{-9}	5.71×10^{-9}	1.08×10^{-9}	1.07×10^{-9}	1.52×10^{-8}	14.1
1.30×10^{-8}	1.33×10^{-8}	2.15×10^{-9}	2.18×10^{-9}	3.65×10^{-8}	16.9
2.96×10^{-8}	3.08×10^{-8}	4.11×10^{-9}	4.20×10^{-9}	8.60×10^{-8}	20.9
6.74×10^{-8}	6.87×10^{-8}	8.41×10^{-9}	8.92×10^{-9}	1.99×10^{-7}	23.6
1.48×10^{-7}	1.53×10^{-7}	1.72×10^{-8}	1.77×10^{-8}	4.41×10^{-7}	25.6
3.26×10^{-7}	3.36×10^{-7}	3.41×10^{-8}	3.38×10^{-8}	9.82×10^{-7}	28.8
7.08×10^{-7}	7.43×10^{-7}	6.93×10^{-8}	7.10×10^{-8}	2.15×10^{-6}	31.1
1.59×10^{-6}	1.64×10^{-6}	1.49×10^{-7}	1.55×10^{-7}	4.87×10^{-6}	32.7
3.13×10^{-6}	3.22×10^{-6}	2.98×10^{-7}	3.05×10^{-7}	9.53×10^{-6}	31.9
6.10×10^{-6}	6.29×10^{-6}	5.96×10^{-7}	6.00×10^{-7}	1.85×10^{-5}	31.1
8.87×10^{-6}	9.16×10^{-6}	9.34×10^{-7}	9.27×10^{-7}	2.67×10^{-5}	28.7
1.80×10^{-5}	1.83×10^{-5}	2.12×10^{-6}	2.21×10^{-6}	5.34×10^{-5}	25.2
2.97×10^{-5}	3.06×10^{-5}	3.98×10^{-6}	4.04×10^{-6}	8.67×10^{-5}	21.8

Figure 4 illustrates the pumping speed curve as a function of pressure for Assembly B. The curve has a characteristic behavior of a 20 L/s SIP⁽⁵⁾ with a peak pumping speed of 32.65 L/s at the pressure of 1.49×10^{-7} mbar. This maximum pumping speed (32.65 L/s) is about 62.5% higher than the nominal speed of the pumping element at this pressure according to⁽⁵⁾. This in part can be explained by the different geometry of the studied element, as can be seen by means of a comparison between the commercial pump and LNLS model (see Fig. 5).

The error among the calculated pressure by Monte Carlo and the measured pressure by the extractor gauges, according to data shown in Table 2, is below 5%. This represents a very good result,

considering the modeling approximations and the pre-defined assumptions⁽⁶⁾ for the Monte Carlo method.

After Monte Carlo's model validation, the analysis was expanded to the Assembly A. The results are shown in Table 3.

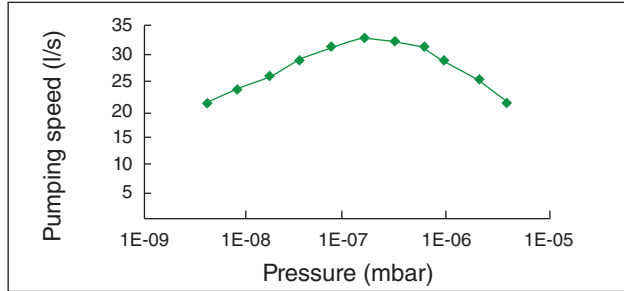


Figure 4: SIP element's pumping speed as a function of pressure (Gauge 2 – Assembly B).

The pumping speed as a function of pressure (gauge 3 of Assembly A set as the reference) is illustrated by Fig. 6. A pumping speed of 13.13 L/s was reached at 4.8×10^{-9} mbar and increased almost linearly until the pressure of 4.7×10^{-8} mbar, when

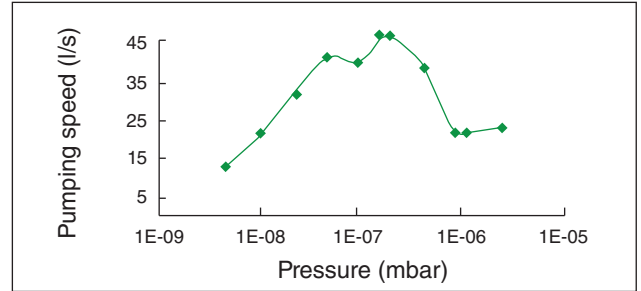


Figure 6: SIP element's pumping speed as a function of pressure (Gauge 3 – Assembly A).

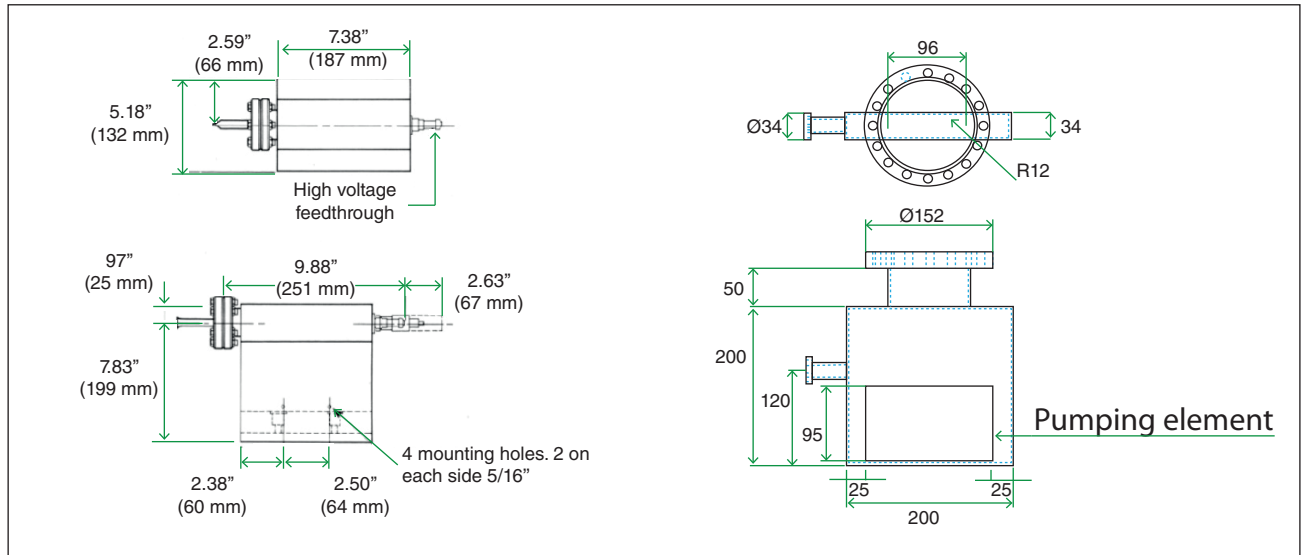


Figure 5: Schematic drawings: (A) commercial 20 L/s SIP and (B) LNLS 20 L/s SIP.

Table 3: Comparison between the calculated pumping speed from measurements and Monte Carlo calculations for Assembly A.

Gauge 1	Gauge 1 MC	Gauge 2	Gauge 2 MC	Gauge 3	Gauge 3 MC	Q	S MC
mbar	mbar	mbar	mbar	mbar	mbar	mbar*L/s	L/s
3.18×10^{-8}	3.24×10^{-8}	1.31×10^{-8}	1.20×10^{-8}	4.80×10^{-9}	4.82×10^{-9}	6.30×10^{-8}	13.1
9.53×10^{-8}	1.03×10^{-7}	3.15×10^{-8}	3.47×10^{-8}	1.02×10^{-8}	1.04×10^{-8}	2.15×10^{-7}	21.1
3.21×10^{-7}	3.47×10^{-7}	1.01×10^{-7}	1.07×10^{-7}	2.30×10^{-8}	2.38×10^{-8}	7.42×10^{-7}	32.3
8.19×10^{-7}	8.93×10^{-7}	2.42×10^{-7}	2.68×10^{-7}	4.73×10^{-8}	4.55×10^{-8}	1.95×10^{-6}	41.1
1.56×10^{-6}	1.73×10^{-6}	4.43×10^{-7}	5.18×10^{-7}	9.47×10^{-8}	9.29×10^{-8}	3.77×10^{-6}	39.9
3.57×10^{-6}	4.00×10^{-6}	9.76×10^{-7}	1.17×10^{-6}	1.87×10^{-7}	1.94×10^{-7}	8.75×10^{-6}	46.7
6.70×10^{-6}	7.39×10^{-6}	1.94×10^{-6}	2.22×10^{-6}	4.12×10^{-7}	4.05×10^{-7}	1.60×10^{-5}	38.9
9.28×10^{-6}	8.79×10^{-6}	3.78×10^{-6}	2.91×10^{-6}	8.50×10^{-7}	8.49×10^{-7}	1.85×10^{-5}	21.9
1.21×10^{-5}	1.18×10^{-5}	4.75×10^{-6}	3.88×10^{-6}	1.12×10^{-6}	1.12×10^{-6}	2.47×10^{-5}	21.9
2.46×10^{-5}	2.61×10^{-5}	8.21×10^{-6}	8.48×10^{-6}	2.40×10^{-6}	2.42×10^{-6}	5.51×10^{-5}	22.9

the pumping speed fell from 41.12 to 39.85 L/s. However, the SIP element's pumping speed increased again and reached the maximum value of 46.66 L/s at 1.87×10^{-7} mbar.

The lower pumping speed attained in low pressure compared with the same pressure for Assembly B, could be attributed to the previous condition of both elements. The element used at Assembly B was new, but the element used at Assembly A was a reconditioned one. This can also explain the different curve behaviors shown on Figs. 4 and 6.

On the other hand, the maximum calculated pumping speed (46.66 L/s) is far higher compared with the obtained pumping speed using Assembly B. One hypothesis to explain this difference is the insertion of the pumping element directly into the vacuum chamber. This different design already gave some enhancement in the pumping speed of Assembly's B SIP element, but was not so evident like in Assembly A. Assembly A has a gas conductance for the pump larger compared with Assembly B. These results were surprising and new experiments must be carried out to better understand them.

Moreover, the error among the calculated pressure by Monte Carlo method and the measured pressures are, for most of points, below 10%, which is good and also found by other authors⁽⁷⁾. However, there are a few points specifically for the gauge 2 of Assembly A that presented an error greater than 15 or 20%. This can be explained by any problem occurred with the gauge or with the obtained calibration factors, which are not constant through the whole pressure range of 10^{-9} to 10^{-6} mbar⁽⁸⁾. The better stability and constancy of the extractor gauges was observed by⁽⁸⁾ and was also proved by the results obtained in the measurements using Assembly B.

CONCLUSIONS

The pumping speed of a 20 L/s SIP element was calculated by different methods aiming the analysis of a distinct assembly design proposed for the vacuum chambers of the SIRIUS storage ring.

The Monte Carlo model was successfully validated by comparison with a standardized chamber (Assembly B) and used

as a reference for the analysis of a vacuum chamber with complex geometry.

The gauge's measured pressures compared to the Monte Carlo's calculations presented a good agreement, with errors less than 10% for most of the evaluated points.

An enhanced pumping speed for both Assemblies A and B was measured. The possibly reason was the increased conductance for the gases to access the SIP elements, which was larger than in a conventional SIP. Further studies will be carried out to better understand this behavior.

REFERENCES

1. LIU, L.; RESENDE, X. R.; RODRIGUES, A. R. D., SIRIUS (Br): A New Brazilian Synchrotron Light Source. IPAC'10 Proceedings, WEPEA006, p. 2481-2483, May. 2010.
2. KERSEVAN, R.; PONS, J. L., Introduction to MOLFLOW+: New graphical processing unit-based Monte Carlo code for simulating molecular flows and for calculating angular coefficients in the compute unified device architecture environment. *Journal of Vacuum Science and Technology A*, v. 27, n. 4, p. 1017-1024, Jul. 2009.
3. HABLANIAN, M. H., Recommended procedure for measuring pumping speeds. *Journal of Vacuum Science and Technology A*, v. 5, n. 4, p. 2552-2557, Jul/Aug. 1987.
4. INTERNATIONAL ORGANIZATION FOR STANDARDIZATION. ISO/DIS 3556-1.2., Sputter-ion pumps – measurement performance characteristics.- part 1: pumps with a volume rate of flow greater than 10 l/s. 1992, 10p.
5. PERKIN ELMER INSTRUCTION MANUAL, Physical Electronics division. Part number 1002393. 28p.
6. SUETSUGU, Y., Application of the Monte Carlo method to pressure calculation. *Journal of Vacuum Science and Technology A*, v. 14, n. 1, p. 245-250, Jan/Feb. 1996.
7. LUO, X.; DAY, C.; HAAS, H.; VAROUTIS, S., Experimental results and numerical modeling of a high performance of a high performance large scale cryopump. I. Test particle Monte carlo Simulation. *Journal of vacuum Science and Technology A*, v.29, n.4, p. ,Jul/Aug 2011
8. LI, D.; JOUSTEN, K., Comparison of the stability of hot and cold cathode ionization gauges. *Journal of Vacuum Science and Technology A*, v. 21, n. 4, p. 937-946, Jul/Aug. 2003.